## A SIMPLE METHOD TO MODEL CRACK PROPAGATION IN CONCRETE

Shahriar Shabazpanahi<sup>1</sup>, Abang Abdullah Abang Ali<sup>2</sup>, Farah Nora Aznieta<sup>3</sup>, Alaleh Kamgar<sup>4</sup>, and Nima Farzadnia<sup>5</sup>

<sup>1</sup> Department of Civil Engineering, University Putra Malaysia, E-mail: sh.shahbazpanahi@gmail.com <sup>2</sup> Housing Research Center, University Putra Malaysia, E-mail: aaaa@eng.upm.edu.my

#### **ABSTRACT**

Crack analysis is vital to explain behavior of concrete structures. In the present study, an interface element with softening spring is used to simulate cohesive zone model (CZM) in beam to accurately explain the propagation for mixedmode crack. Modified crack closure integral method is implemented to model propagation of fracture process zone (FPZ) and stress-free region. An element stiffness matrix is used to derive forces in nodes due to normal and shear stress in the FPZ. Size effects such as depth of the beam, effective crack and initial notch are considered in calculation of the FPZ length and crack extension. By using this model, energy release rate is calculated directly by virtual crack closure technique (VCCT) by considering the variation of work done by external loads. The model decreases computational time and complexity for discrete cracks and provides accuracy as compared to other previous research.

*Keywords*: crack propagation, FPZ, stiffness, energy release rate

### 1. INTRODUCTION

Mechanical behavior of ductile materials is different from that of quasi-brittle materials, e.g., concrete. Cracks grow in metals due to intersection and coalescence of micro-voids, while in concrete, cracks propagate when aggregates interlock and/or when micro-crack bridging occurs.

Modeling of crack in quasi-brittle

#### **REZUMAT**

Analiza fisurării este esentială în explicarea comportării structurilor din beton armat. Pentru a simula modelul zonei coezive (CZM) într-o grindă, în studiul de față este utilizat un element de interfață cu degradare de rigiditate, în scopul explicării corecte a propagării corespunzătoare modului de fisurare mixt. Pentru modelarea zonei procesului de propagare a fisurării (FPZ) și a zonei cu eforturi nule, este implementată metoda integrală modificată de considerare a închiderii fisurilor. În scopul determinării fortelor la nodurile grinzii, datorate eforturilor normale și tangențiale din FPZ, este utilizată o matrice de rigiditate la nivel de element. În calculul lungimii FPZ și al extinderii fisurilor sunt considerate atât efectele dimensiunilor, precum înălțimea grinzii, cât și fisurarea efectivă și amorsarea fisurii. Prin utilizarea acestui model, rata energiei degajate este calculată direct prin tehnica închiderii virtuale a fisurilor (VCCT), prin considerarea lucrului mecanic al solicitărilor exterioare. Modelul utilizat contribuie la scăderea duratei și complexității calculului, pentru fisuri discrete, și este mai precis, în comparație cu alte cercetări anterioare.

Cuvinte cheie: propagarea fisurilor, FPZ, rigiditate, rata energiei degajate

materials is essential to improve reliability and to enhance load bearing. Fracture mechanics was employed to model tensile crack in concrete with strain softening behavior. It was first used to study crack propagation applying linear elastic fracture mechanics (LEFM) in warships in World War II (1). Later some studies used LEFM in concrete propagation analysis, but Kaplan (2) found out that deploying LEFM is not acceptable to solve

<sup>&</sup>lt;sup>3</sup> Department of Civil Engineering, University Putra Malaysia, E-mail: farah@eng.upm.edu.my

<sup>&</sup>lt;sup>4</sup> Department of Civil Engineering, University Putra Malaysia, E-mail: halaleh.kam@gmail.com
<sup>5</sup> Housing Research Center, University Putra Malaysia E-mail: nimafarzadnia@gmail.com

crack problems with normal concrete sizes. Hillerborg et al. (3) proposed the first model in concrete based on nonlinear fracture mechanics. Mentioned study introduces a region, often termed as fracture process zone (FPZ), ahead of real crack tip which leads to crack closure (Fig. 1). This significant and large zone contains micro-cracks in matrixaggregate, gel pores, shrinkage cracks, bridging, and branch of cracks that is located ahead of the macro-cracks. Since a significant amount of energy is stored in this region, a crack can have stable growth before peak load. In addition, the existence of the FPZ justifies the strain softening behavior in the stresscrack opening curve after peak load. In this region, the interlocking crack surfaces after peak load contribute to a gradual decline in stress and prevent sudden failure (1). The FPZ dimension depends on the size of structure, initial crack, loading and material properties of concrete. The length of the FPZ is of special interest as compared to its width. The effective modulus of elasticity is reduced when moving from undamaged regions into the FPZ.

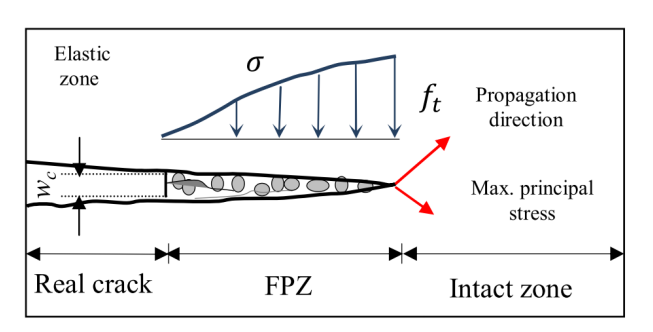


Fig.1. FPZ in front of crack with normal stress

Different approaches have been investigated to model discrete crack as well as its propagation criteria. To simulate the FPZ, Hillerborg et al. (3) used cohesive stress which is a function of crack opening. Hillerborg's approach can be applied to any structure, even if no notch or fictitious crack exists (4). In this model, as stress is a function of crack opening, it reaches tensile strength at the tip of the crack, and reduces to zero at its critical opening  $(w_c)$ . The amount of the area under the stress-crack opening curve is equal to energy release rate. This model, often referred to as cohesive zone model (CZM), was deployed to simulate the FPZ in normal size structures, using either nodal force release method or interface element with zero initial thickness technique (5).

Also, Bazant and Oh (6) modeled the FPZ in dummy bands as if micro-cracks are distributed uniformly in constant opening. This model, called crack band model (CBM), is used in finite element method with a layer continuum element. The CBM depends on the width of the element and it has been suggested only to model Mode I fracture (7).

Non-local continuum approach is another method that uses width and length for modeling FPZ but it has too many degrees of freedom, and for this reason, it is not computationally affordable (8).

Other models were proposed based on LEFM such as size-effect model (9), two-parameter fracture model (10) and effective crack model (11). Some user friendly models were modified using the concept of LEFM such as  $K_R$ -curve method (12) regarding to cohesive forces in FPZ and double-K fracture model (13) based on using a weight function. Recently the double-G fracture model (14) was introduced based on energy release rate in which the rate deals with Young's modulus, crack length and member geometry. The last three methods listed have singularity problems in boundary integrals, which need specific numerical methods (15).

far, the method suggested by Hillerborg et al. (3) has been applied more widely due its practicality, accuracy and cost effectiveness. To model the CZM, two types of interface elements were deployed. One of the most widely used interface element is continuum cohesive zone model (CCZM) (e.g. Xie and Gersle (16)). An alternative interface element is the discrete cohesive zone model (DCZM), which is very simple to implement (17). The DCZM results are satisfactory compared to CCZM, especially for precracking phase when stiffness is selected to have a very large value (18). The DCZM is based on the idea that cohesive zone behaves like a spring. This point of view suggests that

instead of using a 2-D interface element along the crack path, a spring element should be utilized between interfacial node pairs. In the present investigation, DCZM is applied, because this method reduces computational time and is compatible with the finite element method (19).

One of the methods for crack propagation modeling in the DCZM is the virtual crack closure technique (VCCT). In this method, the energy release rate is calculated directly, and then is compared with the crack resistance. Energy for the closing crack was calculated by multiplying the nodal force displacement opening (20). If the energy release rate is larger than the crack resistance, then the crack grows. Rybicki and Kanninen (21) for the first time suggested this method and Raju (22) improved the approach. This method is computationally inexpensive and provides satisfactory results (23).

Another issue in cracking modeling is crack direction. The initial direction of propagation is usually unknown. For crack growing, many researchers proposed to use approximate re-meshing algorithms. In these algorithms, a significant number of nodes are created for re-meshing, thereby resulting in creating large stiffness matrices, splitting some of the elements, and increasing computational complexity and time. An alternative method is the inter-element boundaries technique, which directs the crack path (24). In this technique, the crack follows the existing inter-element boundaries; no re-meshing algorithm is needed.

From the finite element point of view, the stiffness of element should be properly chosen. In previous research, element stiffness was estimated from the Young's modulus (18) to model FPZ propagation. In practice, this damage zone has a different stiffness due to micro-cracking, bridging, branching undertake use of energy in crack growth. So it is significant to use more accurate stiffness element to simulate the FPZ in finite element method. This can be obtained from the softening curve, for that the stiffness of the FPZ is smaller than Young's modulus. Also, when the FPZ length is fully extended and

arrived at the maximum rate, stress-free length is appears in front of notch or macro-crack, behind FPZ, (25) which was not considered by previous research (26, 27, 16, 28, 5, 17, 29).

Also, to predict crack propagation, correct estimation of energy release rate is important. As it is known, energy release rate is the basic idea of nonlinear fracture mechanics for crack propagation that depends on many parameters such as size of structure, external load, element stiffness and FPZ length. Thus, it is necessary to consider more accurate element stiffness, effect of external load and FPZ length to evaluate energy release rate.

In the present study, interface element boundaries are utilized to simulate cohesive cracks. This model justifies the softening behavior of normal stress in two dimensional finite element methods in beam. Modified crack closure integral method with softening spring is applied. A spring element stiffness matrix is used to derive forces in nodes due to normal and shear stress in the FPZ. Size effect such as depth of the beam, effective crack, initial notch are considered in FPZ to estimate energy release rate. Also, variation of FPZ length is utilized to model crack propagations. Strain energy release rate is obtained directly from variation of work done by externally applied loading. Instead of re-meshing, this work uses a method which finds the crack propagation direction by following interface element boundaries (24). Results for two examples are presented and comparisons between computed and experimental recent results are made.

# 2. NUMERICAL MODEL

The model used in the present study has some differences as compared to other available DCZM. It uses a softening spring stiffness matrix to model crack extension as FPZ length changes in the beam. It considers the variation of work done by externally applied loads to estimate total energy release rate.

# 2.1. Interface element

Modified crack closure integral method is applied to model CZM (19) for mixed-mode.

As mentioned before, the FPZ has a softening action due to the interlock of aggregates and micro-cracks. Thus, a nonlinear spring is proposed to place between interfacial node pairs (Fig. 2). In this figure, the node pairs '1' and '2' have initially the same coordinates. Spring softening is set at the crack tip between the nodes '1' and '2'. Node '3' is a dummy node and it is only used to illustrate the variation in the crack form.

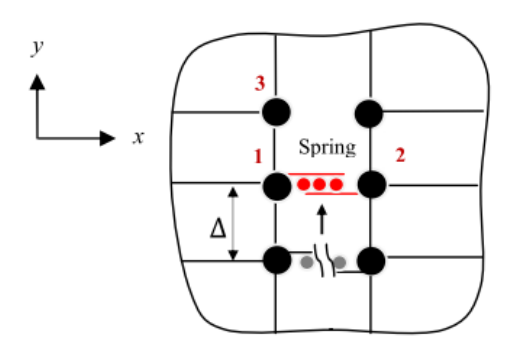


**Fig. 2.** Spring interface element between two nodes

The local element stiffness matrix and the displacement vector related to nodes '1' and '2' are given by (19):

$$\mathbf{K} = \begin{bmatrix} k_{x} & 0 & -k_{x} & 0 \\ 0 & k_{y} & 0 & -k_{y} \\ -k_{x} & 0 & k_{x} & 0 \\ 0 & -k_{y} & 0 & k_{y} \end{bmatrix}, \mathbf{u} = \begin{bmatrix} u_{1} \\ u_{2} \\ u_{3} \\ u_{4} \end{bmatrix}$$
(1)

where  $k_x$  and  $k_y$  are the stiffness values corresponding to the local coordinates x and y, respectively,  $u_1$  and  $u_2$  are displacement components in x and y directions for node '1',  $u_3$  and  $u_4$  are displacement components in x and y directions for node '2', respectively. In this research, the value of the stiffness in x direction,  $k_x$ , is based on the normal stress versus crack opening curve. Fig. 3 illustrates the concrete crack opening displacement (COD) that was proposed. The behavior initially is elastic and then it becomes softening. In the softening zone, there is still some resistance, but stress drops dramatically.

The total crack opening can be separated into two components:

$$dw = dw_e + dw_s \tag{2}$$

where  $dw_e$  and  $dw_s$  are the elastic opening and softening opening, respectively. The softening parameter is defined as:

$$S = -\frac{d\sigma}{dw_s} \tag{3}$$

This parameter indeed is the slope of stress in softening portion of the curve and its value is negative. If  $S_e$  and  $S_s$  are the slopes in the elastic and softening zones, respectively, then:

$$S_e = \frac{d\sigma}{dw_e} \quad , \quad S_s = -\frac{d\sigma}{dw} \tag{4}$$

Substituting Eq. (4) into Eq. (3), the softening parameter is defined as:

$$S = -\frac{d\sigma}{dw - dw_e} = \frac{S_S}{1 + \frac{S_S}{S_e}}$$
 (5)

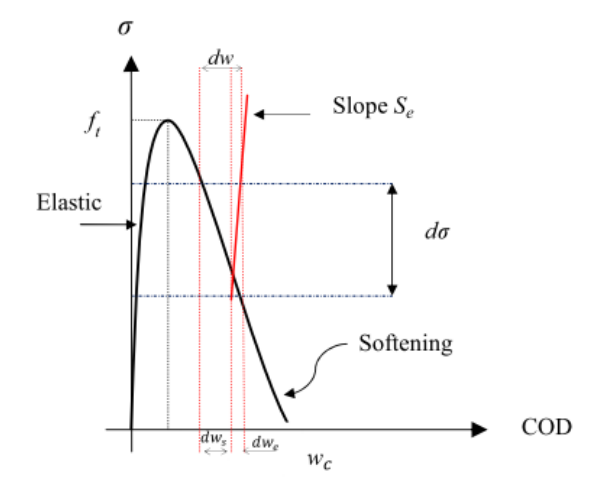


**Fig. 3.** Concrete  $\sigma$  –COD curve

Also, the spring stiffness can be expressed by:

$$k_{s} = B\Delta \frac{d\sigma}{dw} = B\Delta \frac{d\sigma}{\frac{d\sigma}{S_{e}} + \frac{d\sigma}{S_{s}}}$$
 (6)

where B is the thickness of the beam and  $\Delta$  is the element size. From Eq. (5) and (6), it results that:

$$k_x = B\Delta \left(S_e - \frac{S_e^2}{S_e - S}\right) \tag{7}$$

Shear stress transfers by fracture zone in the tip of crack that it is required to be modeled by interface element. Experimental formulation is applied by Jeang and Hawkins (30) to consider aggregate interlock. The stiffness component in y direction is considered as (30):

$$k_{v} = GB \left[ 1 - e^{-\left[0.262 \left(1/\Delta u'\right)^{1.5} - 17.17\right]10^{-4}} / 25.4 \right] (8)$$

where G is the shear modulus and  $\Delta u'$  is the maximum crack opening displacement. Since Bazant and Gambarova (31) assumed that slip occurs opening after displacement, maximum crack opening displacement in Eq. (8) is assumed critical value,  $w_c$ .

The angle of orientation  $(\theta)$  of element is (Fig. 4):

$$\cos\theta = \frac{x_3 - x_1}{\sqrt{(x_3 - x_1)^2 + (y_3 - y_1)^2}}$$
 (9)

where  $x_1$  and  $y_1$  are the coordinates of components node '1' and  $x_3$  and  $y_3$  are coordinates of components node '3'.

In this investigation direction of crack is implemented by a method in which crack goes after existing inter-element borders. This method has simple algorithm and there is no need for re-meshing. Crack propagation follows one of inter-elements (AB) or (AC) at which it is assumed that crack will not stop and intersect the main element (Fig. 4). There are two possible cases for the crack path; if the

orientation angle  $(\theta)$ , is less than  $45^{\circ}$ , the path of growth is AB, otherwise it will be AC. Although crack paths are non-smooth, the ones found with this method give a good agreement with correct crack path.

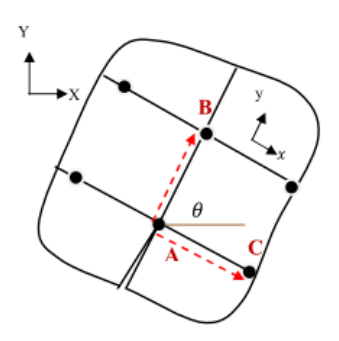


**Fig. 4.** Two possible cases for the direction of propagation

The stiffness matrix, nodal forces and displacements can be changed in local (x, y) system to global system (X, Y) by using the transformation matrix (19).

# 2.2. Energy release rate

The nodal force  $(F_x)$  due to strain energy in x direction is:

$$F_x = k_x \left( u_1 - u_3 \right) \tag{10}$$

The crack opening displacement is calculated by using displacements of dummy nodes 3 and 4 (which do not contribute to the stiffness matrix) as:

$$\Delta u = u_5 - u_7 \tag{11}$$

where  $\Delta u$  is the crack opening displacement while  $u_5$  and  $u_7$  are displacement components in x direction for nodes 3 and 4, respectively.

Strain energy release rate for mixed-mode in concrete is assumed to be the same as Mode I magnitude (27). Strain energy release rate for Mode I, due to this force based on VCCT, is (23):

$$\frac{\partial U}{\partial A} = \frac{F_x \Delta u}{2BL'} \tag{12}$$

where A is crack surface area and L' is crack extension.

In the present study, the variation of work done by externally applied loading is used to estimate energy release rate. If  $F_x$  is nodal force due to external load in x direction, then:

$$\frac{\partial U}{\partial A} = \frac{F_x(u_1 - u_3)}{2BL} \tag{13}$$

where W is the work done by the externally applied load. Therefore, the energy release rate,  $G_1$  for Mode I is:

$$G_{I} = \frac{\partial U}{\partial A} - \frac{\partial W}{\partial A} = \frac{F_{x} \Delta u}{2BL} - \frac{F_{x} (u_{1} - u_{3})}{2BL}$$
(14)

This value is compared with critical strain energy release rate  $(G_c)$  for crack propagation. Eq. (14) can be applied for mixed-mode and multiple-crack fracture problems.

## 2.3. Crack extension and FPZ length

The crack extension has an essential significance in fracture mechanics and is based on FPZ length (32). It was shown that crack extension has linear relation with FPZ length until crack opening displacement reaches to  $3.6\,G_c\,/\,f_t$  where the  $f_t$  is tensile strength of concrete. After that, as crack extension increases, FPZ length decreases. Thus, crack extension is:

if 
$$\Delta u \ll 3.6 \frac{G_{IC}}{f_t}$$
:  $L' = l_p (h - a_0)$  (15.a)

if 
$$\Delta u > 3.6 \frac{G_{IC}}{f_t}$$
:  $L = -0.1 l_p (h - a_0)$  (15.b)

where h and  $a_0$  are the depth of the beam and the length of the initial notch. So, to estimate crack extension, an exact criterion for FPZ length is necessary. In the present study, Xu *et al.*'s approach (33) is used to evaluate FPZ length. Fig. 5(a) shows effective crack, in which  $l_p$ ,  $a_{\sigma=0}$  and a are FPZ length,

stress-free region length and effective crack length, respectively.

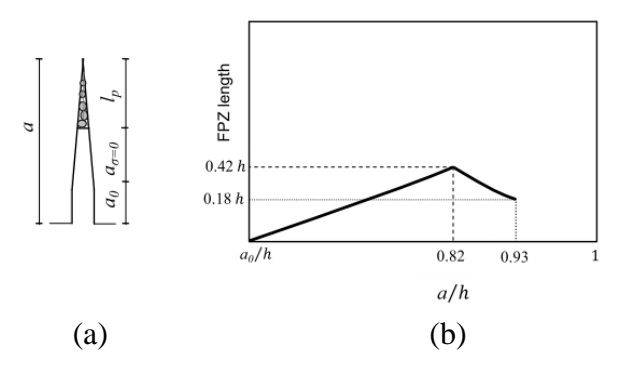


**Fig. 5.** (a) Effective crack length, (b) Variation of FPZ length (33)

Fig. 5 (b) illustrates linear relationship between FPZ length and effective crack length (33). Length of FPZ increases up to the maximum value, 0.42h at a = 0.82h, and then decreases until it reaches the value 0.18h at a = 0.93h. The advantage of the present model is that the effect of size on FPZ length based is considered on the above-mentioned approach. A more accurate explanation of propagation and crack formation must be considered in model such as stress-free region length that is formulated in finite element methods by:

$$a_{\sigma=0} = N \times \Delta \tag{16}$$

where *N* is the number of elements that have failed behind crack. When FPZ has fully propagated, the *N* element is set to zero behind the crack and the crack grown along the respective element with considering direction at each step.

# 2.4. Computer implementation

The FEAPpv program code is developed for the analysis of 2-D plane stress in concrete (34). A nonlinear spring is implemented for the interface element in the Fortran User Subroutine FEAPpv, while the nonlinear dynamic relaxation method is used for the interface element (16). Four-node isoparametric elements are used for bulk concrete considered as linear elastic. Initially,

 $k_x$  and  $k_y$  are chosen with very large values to ensure that the crack is still closed. For crack stability,  $k_x$  and  $k_y$  are computed according to Eq. (7) and (8). Crack does not propagate when the energy release rate,  $G_I$ , is smaller than the critical strain energy release rate  $(G_c)$ . Fig. 6 shows the major steps used by the presented numerical model to solve fracture in the beam.

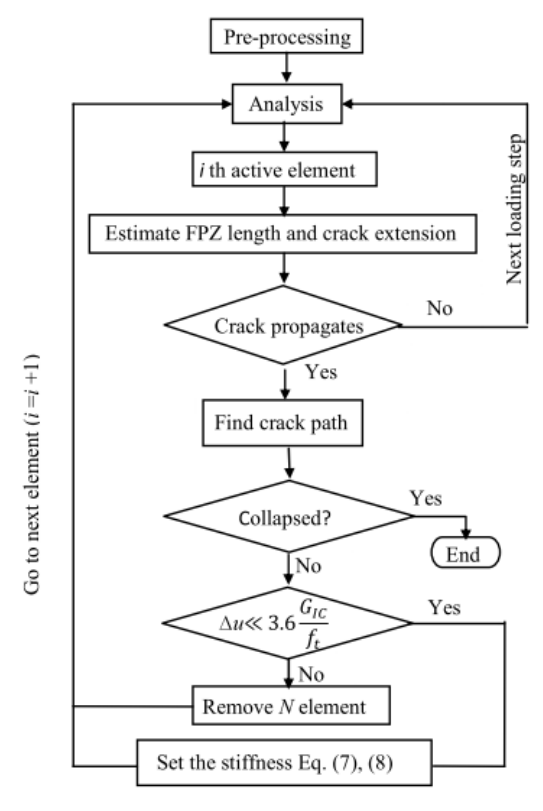


Fig. 6. Flowchart of fracture in the i-th element

### 3. RESULT AND DISCUSSION

Fig. 7 shows the tested plain four-point single-edge notched shear (SENS) beam tested (26). Material properties of concrete are 24800 MPa Young's modulus, 0.18 Poisson's ratio and 4 MPa tensile strength. The thickness of the beam is 152 mm and the length of the initial notch is 82 mm. Parameter values for fracture are  $G_c = 150N/m$ ,  $w_c = 0.135$  mm and  $w_0 = 0.0001$  mm. The initial mesh (c) is illustrated in Fig. 7 (b). The dimension of the elements is selected very small in the area of possible cracking to better look for results.

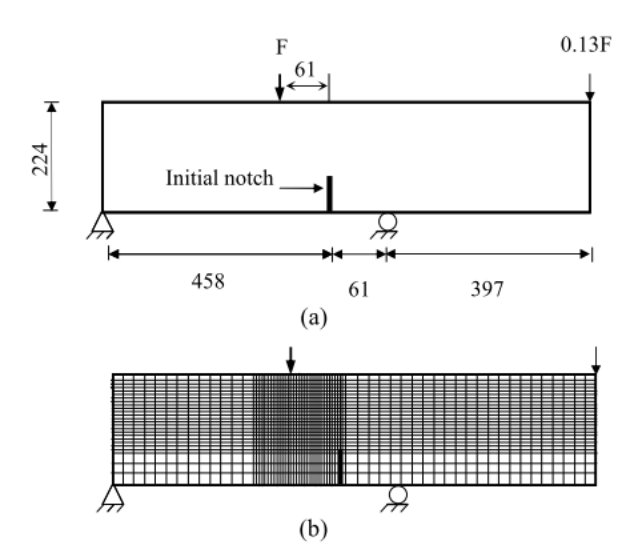


Fig.7. Beam with notched shear: (a) Geometry (units: mm) (b) Initial mesh

Fig. 8 indicates load versus crack mouth sliding displacement (CMSD) curve with three size meshes compared with experimental envelop (26) and a model by Xie and Gerstle (16). Mesh (a) have 864 elements and 324 interface elements, mesh (b) have1026 elements and 508 interface elements, and (c) have 1862 elements and 875 interface elements.

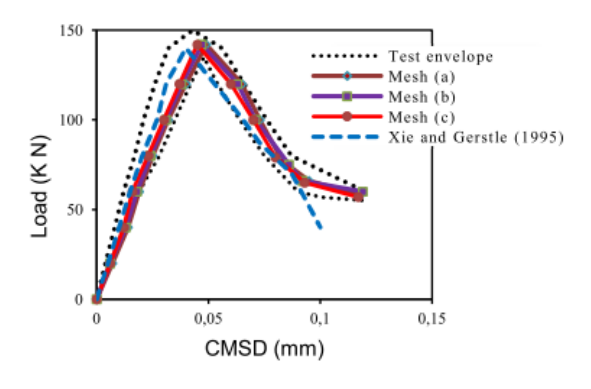


Fig. 8. Load-CMSD Curves for Shear Beam

The approximate matching of the three curves demonstrates the independence of the model from mesh size and shows the model has fast convergence. It can be seen from the figure that peak loads are close to each other, although mesh size is changed.

As seen, the numerical results are logical regarding to experimental envelope. In the elastic part, the results rest almost on the midpoint of previous experimental. However, peak load obtained from the numerical method

is slightly shifted to right upper limit of the envelope. The difference between proposed model and experimental data is inevitable since the behavior of concrete is assumed linear elastic in fracture mechanics but in fact it is nonlinear plastic and compression cracking is also ignored.

The peak loads have 5.4% difference compared with experimental ones. It is seen that after peak load, the curves in the softening zone (up to 60 KN) are closer to experimental data than the previous numerical (16) model, which is slightly more brittle thereafter. In the softening zone after 60 KN, present model shows more agreement in terms of ductility observed in experimental than previous study. It is may be because that stress-free zone at the tip of the notch was not considered in modeling.

Fig. 9 shows the predicted crack path in mesh (c) which is compared with test. It should be noted that, crack path is a smooth curve although in present study crack path consists of two straight line. It can be seen that prediction of crack path in mesh (c) is very close to the experimental (up to 95%).

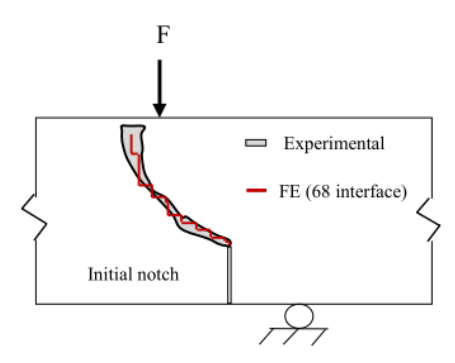


Fig. 9. Crack path in the shear beam

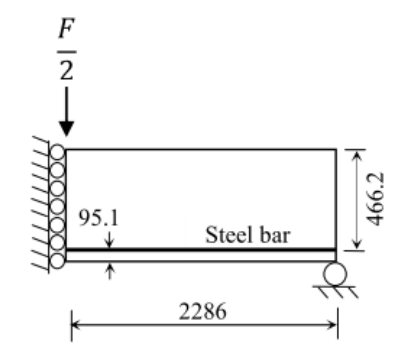
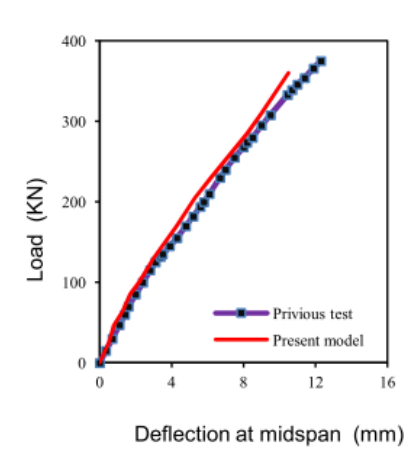


Fig.10. Half of the RC Beam (Unit: mm)

The second example is a reinforced concrete beam with simple supports (Fig. 10) which was tested by Bresler and Scordelis (35).

The geometry of the RC beam is 4572 mm length, 305.8 mm thickness. Material properties are: 24000 MPa elastic module, 0.18 Poisson ratio for concrete and 200 GPa elastic module, 0.3 Poisson ratio, 3290 cross-section area, 552 MPa yield strength for steel. Tensile strength for concrete is 2.8 MPa and critical crack opening displacement is 0.152 mm. A two-node truss element is used to model steel bars with perfect plastic behavior and the beam is not reinforced with stirrups. The analysis condition is considered plane stress and half of the beam is simulated for modeling in symmetry condition. Bond-slip between longitudinal bars and concrete is perfect. Load versus deflection at the middle of the beam in present study is compared with experimental results (35) in Fig. 11.



**Fig.11.** Load-deflection at the mid-span of the model and experimental (35)

Fig. 11 shows that the results are close to experimental data. It can be seen that the stiffness in the present study is slightly greater than that from experimental observation (with approximately 10 percent). This error may be because compression acceptable cracks, nonlinear behavior of bulk concrete and plastic deformation are neglected in fracture mechanics. Fig. 12 (a) shows crack patterns at load equal to 285 KN in the experimental study (35) and Fig. 12 (b) illustrates crack

paths in the present study. Flexural cracks occur under load initially. Effective crack length is 10.2 mm and occurs at load 54 KN in the vicinity of the mid-span and becomes 262.7 mm at 100 KN load. Shear cracking starts at about 170 KN load at the support and grows upwards as load increases.

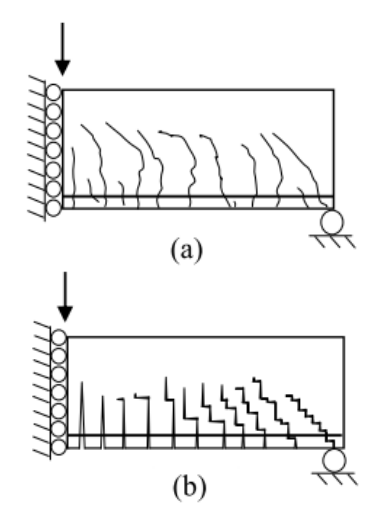


**Fig.12**. Crack predicted at 285 KN load (a) experimental (35); (b) present model

The experimental model showed 13 cracks, including flexural and shear cracks which, except the first one, are inclining toward the load, while in the present model 11 cracks were predicted, in which two cracks near mid-span don't detour.

## 4. CONCLUSIONS

The present investigation proposes a simulate simple approach to cohesive cracking. An interface element with a softening spring is used to simulate CZM in beam to accurately explain crack propagation for mixed-mode cracking. A modified crack closure integral method is implemented to simulate the development of FPZ and the stress-free region length of fracture without re-meshing. An accurate element stiffness matrix is applied to derive forces in nodes due to normal and shear stress in this zone. Depth of the beam, effective crack and initial notch are considered in FPZ and in crack extension assessment. By using this model, the energy release rate is calculated directly by VCCT, by considering the variation of work done by externally applied loads. The model is simple, accurate, efficient, with fast convergence and capable to accurately model the crack growth. The model decreases computation time and complexity for discrete cracks and provides accuracy by comparison with previous research.

### **REFERENCES**

- 1. ESFAHANI, M. R., *Fracture mechanics of concrete*, Tehran Polytechnic press, Tehran Iran, 2007.
- 2. KAPLAN, M. E., *Crack propagation and the fracture concrete*, American Concrete Institute, ACI, 58 (5), 591-610, 1961.
- 3. HILLERBORG, A., MODEER, M., PETERSSON, P. E., Analysis of crack formation and crack growth in concrete by means of mechanics and finite element, Cement and Concrete Research, 6, 773-782, 1976.
- 4. ANDERSON, T. L., Fracture mechanics fundamental and application., CRC Press Inc., Boca Raton, FL, 1991.
- 5. YANG, Z. J., LIU, G. Towards fully automatic modelling of the fracture process in quasi-brittle and ductile materials: a unified crack growth criterion, Journal of Zhejiang University Science A, 9 (7), 867-877, 2008.
- 6. BAZANT, Z. P., OH, B. H. *Crack band theory for fracture of concrete*, Materials and Structures, 16 (3), 155-177, 1983.
- 7. ROTS, J., Brost, R. D., *Analysis of mixed-mode fracture in concrete*, Journal of Engineering Mechanics, 113 (11), 1739-1758, 1987.
- 8. INGRAFFEA, A. R., GERSTLE, W. H., GERGELY, P., SAOUMA, V., Fracture mechanics of bond in reinforced concrete, Journal of Structural Engineering, 110 (4), 1871-1890, 1984.
- 9. BAZANT, Z. P., Size effect in blunt fracture: Concrete, rock, metal, Journal of Engineering Mechanics, ASCE, 110 (4), 518-535, 1984.
- 10. JENQ, Y. S., SHAH, S. P. A, two parameter fracture model for concrete, Journal of Engineering Mechanics, 111 (4), 1227-1241, 1985.
- 11. NALLATHAMBI, P., KARIHALOO, B. L., Determination of specimen-size independent fracture toughness of plain concrete, Magazine of Concrete Research, 38 (135), 67–76, 1986.
- 12. XU, S., REINHARDT, H. W., Crack extension resistance and fracture properties of quasi-brittle materials like concrete based on the complete

- process of fracture., International Journal of Fracture, 92, 71–99, 1998.
- 13. XU, S., REINHARDT, H. W., Determination of double-K criterion for crack propagation in quasibrittle materials, part I: Experimental investigation of crack propagation, International Journal of Fracture, 98, 111–149, 1999a
- 14. XU, S., ZHANG, X., Determination of fracture parameters for crack propagation in concrete using an energy approach, Engineering Fracture Mechanics, 75, 4292–4308, 2008.
- 15. KUMAR, S., BARAI, S. V., Concrete fracture models and applications, Springer, Berlin Heidelberg, 2011.
- 16. XIE, M., GERSTLE, W. H., Energy-based cohesive crack propagation modeling, Journal of Engineering Mechanics, ASCE, 121 (12), 1349-1458, 1995.
- 17. SHI, Z., Crack analysis in stuctural concrete, theory and aplication, Butterworth-Heinemann, Burlington, 2009.
- 18. XIE, D., WAAS, A. M., Discrete cohesive zone model for mixed-mode fracture using finite element analysis, Engineering Fracture Mechanics ,73 ,1783–1796, 2006.
- 19. XIE, D., SALVI, A. G., SUN, C., WAAS, A. M., CALISKAN, A. I., Discrete Cohesive Zone Model to Simulate Static Fracture in 2D Triaxially Braided Carbon Fiber Composites, Journal of Composite Materials, 40(22), 2025-2046, 2006.
- 20. TOUDESHKY, H. H., HOSSEINI, S., MOHAMMADI, B., Progressive delamination growth analysis using discontinuous layered element, Composite Structures, 92, 883–890, 2010.
- 21. RYBICK, E. F., KANNINEN, M. F., A finite element calculation of stress intensity factors by a modified crack closure integral, Engeneering Fracture Mechanics, 9, 931–938,1977.
- 22. RAJU, I. S., Calculation of strain-energy release rates with higher orde rand singular finite elements, Enineering Fracture Mechanics, 28, 251–274, 1987.
- 23. XIE, D., BIGGERS, S. B. J., *Progressive crack growth analysis using interface element based on the virtual crack closure technique*, Finite Elements in Analysis and Design, 42 (11), 977 984, 2006.

- 24. ALFAIATE, J., PIRES, E. B., MARTINS, J. A. C., A finite element analyss of non-prescribed crack propagation in concrete, Composite Structure, 63 (1), 17-26, 1997.
- 25. WUA, Z., RONG, H., ZHENG, J., XU, F., An experimental investigation on the FPZ properties in concrete using digital image correlation technique, Engineering Fracture Mechanics, 78 (17), 2978–2990, 2011.
- 26. ARREA, M., INGRAFFEA, A. R., *Mixed-mode crack propagation in mortar and concrete*, Report No. 81-13, Department of Structural Engineering, Cornell University, 1982.
- 27. BOCCA, P., CARPINTERI, A., VALENTE, S., *Mixed-mode fracture of concrete*, International Journal of Solid and Structures, 27 (9), 1139-1153, 1991.
- PRASADA, M. V. K. V., KRISHNAMOORTHY, C. S., Computational model for discrete crack growth in plain and reinforced concrete, Computer Methods in Applied Mechanics and Engineering, 191, 2699–2725, 2002.
- 29. GUO, X., SU, R. K. L., YOUNG, B., Numerical Investigation of the Bilinear Softening Law in the Cohesive Crack Model for Normal-Strength and High-Strength Concrete, Advances in Structural Engineering, 15 (3), 373-388, 2012.
- 30. JEANG, F. L., HAWKINS, N. M., *Non-linear analysis of concrete fracture*, Report No. SM 85-2, University of Washington, USA, 1985.
- 31. BAZANT, Z.P., GAMBAROVA, P., *Rough cracks in reinforced concrete*, Journal of the Structural Division, 106(4), 819–842, 1980.
- 32. ZHANG, D., WU, K., Fracture process zone of notched three-point-bending concrete beams, Cement and Concrete Research, 29(12), 1887–1892, 1999.
- 33. XU, F., WU, Z., Zheng, J., ZHAO, Y., LIU, K., Crack extension resistance curve of concrete considering variation of FPZ length, Journal of Materials in Civil Engineering, ASCE, 23 (5), 703-710, 2011.
- 34. TAYLOR, L. R., *FEAPpv source*, *A finite element analysis program*, *Personal version*, University of California, Berkeley, 2009.
- 35. BRESLER, B., SCORDELIS, A. C., *Shear strength of reinforced concrete beams*, American Concrete Institute, ACI, 60 (40), 51-72,1963.